Kinetics and Catalysis, Vol. 41, No. 4, 2000, pp. 538–545. Translated from Kinetika i Kataliz, Vol. 41, No. 4, 2000, pp. 593–600.
Original Russian Text Copyright © 2000 by Zaikovskii, Chesnokov, Buyanov, Plyasova.

Formation of Filamentous Carbon from 1,3-Butadiene over a Ni–Pd/Al_2O_3 Catalyst

V. I. Zaikovskii, V. V. Chesnokov, R. A. Buyanov, and L. M. Plyasova

Boreskov Institute of Catalysis, Siberian Division, Russian Academy of Sciences,
Novosibirsk, 630090 Russia

Received February 3, 1999

Abstract—The formation of carbon filaments from 1,3-butadiene over a Ni–Pd/Al_2O_3 catalyst at 400–450°C was studied by high-resolution electron microscopy and X-ray diffraction analysis. The carbon filaments differ in morphology and in the arrangement of active metal inclusions: (1) abundant ~ 1000 Å thick filaments contain biconical alloy particles in the middle of the filament, (2) thin filaments of a thickness less than 500 Å rolled in helical fashion contain oval-shaped alloy particles in the middle, and (3) in a few filaments that are less than 200 Å thick, alloy particles are positioned at the ends. When the first two types of filaments grow, decomposition of the hydrocarbon occurs at the active sites of the surface with the formation of a carbide microphase with a hexagonal structure. This phase is called the active microphase. When the reaction stops, the active phase decomposes to form carbon and hexagonal nickel. Extensive defects like grain boundaries and stacking fault dislocations are present in the bulk of Ni–Pd alloy particles. The origin of these defects is related to the epitaxial effect of the active microphase particles on the alloy.

INTRODUCTION

Graphite filaments formed by the catalytic decomposition of hydrocarbons over the particles of some metals and alloys possess a set of interesting properties and have attracted widespread attention in the past few years. Previously [1, 2], it was found that filamentous graphite forms by a “carbide cycle” mechanism. A key point of this mechanism is hydrocarbon decomposition over the microparticles of the iron subgroup metals and their alloys with some other metals to form a metastable carbide compound. When the latter decomposes, carbon atoms arise which diffuse through the metal particle to the nuclei of a graphite phase formed.

The composition and properties of the catalyst particles, as well as the conditions of catalyst preparation, markedly affect the morphology and structure of the filamentous carbon. In some cases, the filaments in the form of spirals [3, 4] and “octopuses” [5–7] arise along with usual straight-line filaments. The regularities and mechanisms of the formation of straight filaments and filamentous octopus-like species have been described in [8, 9]. The reasons for the formation of helical filaments are unknown.

EXPERIMENTAL

Catalysts were prepared* by the mechanochemical activation of NiO, $PdCl_2$, and $Al(OH)_3$ powders. The reduction and carbonization deposition of a sample with the composition 73 wt % Ni + 18 wt % Pd + 9 wt % Al_2O_3 were carried out in a reactor equipped with a McBain balance. The catalyst was reduced by heating it in a hydrogen flow up to 550°C for 20–30 min followed by cooling to a specified temperature of carbonization. The Ni–Pd/Al_2O_3 catalyst was carbonized at 450°C in a medium of 1,3-butadiene diluted by argon and hydrogen in the molar ratio $C_4H_6 : H_2 : Ar = 2 : 40 : 75$. Carbonization did not occur at the temperatures of 350 and 400°C under these conditions. Therefore, in the experiments at 400°C, the hydrogen content of the reaction medium was decreased ($C_4H_6 : H_2 : Ar = 2 : 10 : 75$), and hydrogen was not used at all at 350°C ($C_4H_6 : H_2 : Ar = 2 : 0 : 75$).

After carbonization, the samples were examined on a JEM-2010 electron microscope with a resolution of 1.4 Å with respect to the lattice and at an accelerating voltage of 200 kV. A goniometer was used to obtain images with a given orientation of crystals.

X-ray diffraction patterns were recorded on a URD-63 diffractometer (Germany) with the use of CuK_α radiation and a graphite monochromator. The lattice parameters were measured using the Ni (311) line with an accuracy of ±0.001 to ±0.003 Å, depending on dispersion. The composition of Ni–Pd alloys was determined on the assumption that the lattice parameters of the alloys of isostructural metals undergo a linear change. According to data from the ICSD databank, Ni and Pd crystals exhibit an fcc lattice with the parameters $a = 3.5238$ and $a = 3.8898$ Å, respectively. The particle size D (a size of the coherent-scattering region) was determined by the Selyakov–Scherrer formula [10, 11] for the (111) line, with an accuracy of ±5%.

---

* We are grateful to V.V. Molchanov for preparing the catalyst samples.

0023-1584/00/4104-0538$25.00 © 2000 MAIK “Nauka/Interperiodica”

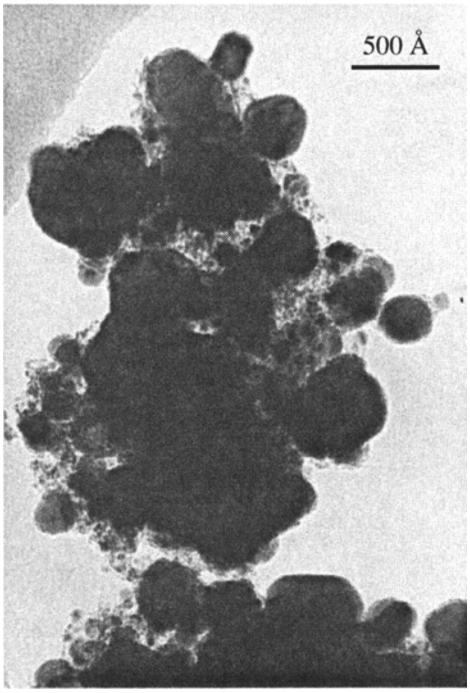

Fig. 1. Ni–Pd alloy particles in the starting sample after the reduction in H_2 at 550°C.

RESULTS AND DISCUSSION

X-ray Diffraction Data

According to the XRD data, the phase of a cubic Ni–Pd alloy (see the table) whose composition depends on the carbonization temperature occurs in both reduced and carbonized samples. As follows from the table, the system is separated into the alloys of two compositions, which are more and less rich in palladium, even upon reduction. This effect is due to the redistribution of Pd in the bulk of particles, which is accompanied by the enrichment of the surface in the metal [12].

After carbonization of the catalyst at 350°C in a medium of 1,3-butadiene diluted with argon, the phase composition of the sample was changed only slightly. Both of the alloys were retained; however, the palladium distribution between them was more uniform.

Carbonization at 400°C results in a substantial redistribution of palladium: both alloys become enriched in palladium and a noticeable amount of a third phase of hexagonal nickel appears. When the carbonization temperature is further increased up to 450°C, only one alloy remains, with a Pd content of 14 at. %. Hexagonal nickel is not detected in this sample.

Electron Microscopy Data

The starting sample reduced in hydrogen at 550°C. This sample is a mixture of poorly faceted Ni–Pd alloy crystals with sizes from 100 to 2000 Å separated by finely dispersed alumina, γ-Al_2O_3 (Fig. 1).

Carbonization at 350 and 400°C. Carbon layers with a thickness of 20 to 200 Å, which cover the surface of alloy particles with a size of 500 Å or higher, form at a temperature of 350°C (Fig. 2). A fraction of the surface of the alloy particles remains uncovered with carbon and, consequently, is capable of exhibiting the catalytic activity in the hydrocarbon decomposition.

At 400°C, two carbon branches begin to grow in different directions on irregularly shaped metal particles ranging in size from 300 to 1000 Å (Fig. 3). Carbon-free regions of the metal surface occur between these branches. Thin (~200 Å thick) carbon filaments containing active metal particles at the ends were also formed. According to the XRD data (see the table), hexagonal nickel prevails in the cooled sample. More finely dispersed particles consist of a Ni–Pd alloy enriched in palladium as compared to the starting uncarbonized sample. As is well known [13], the metastable nickel carbide Ni_3C forms by the interaction between nickel metal and butadiene at temperatures of 300–350°C. The formation of Ni_3C has been found upon the interaction between Ni and CO in the temperature range 300–400°C [14]. Therefore, the appearance of hexagonal nickel in the Ni–Pd/Al_2O_3 catalyst sample carbonized at 400°C can be due to the formation of Ni_3C during the reaction and the decomposition of this carbide to the metal and carbon on cooling the sample. The above data allow one to assume that the carbide Ni_3C is the active phase in the course of the carbonization of the sample at 400°C.

Phase composition of the Ni–Pd/Al_2O_3 catalyst according to XRD data

Carbonization temperature, °C	Carbon content, wt %	Phase composition	Unit cell parameter, Å	Crystallite size, Å	Pd content of alloy, at. %
Starting sample	0	Ni–Pd alloy	$a = 3.542$	100	5
		Ni–Pd alloy	$a = 3.593$	100	19
400	63	Ni–Pd alloy	$a = 3.548$	140	7
		Ni–Pd alloy	$a = 3.620$	100	26
		hexagonal Ni	$a = 2.633$	250	
			$c = 4.330$		
450	100	Ni–Pd alloy	$a = 3.575$	95	14

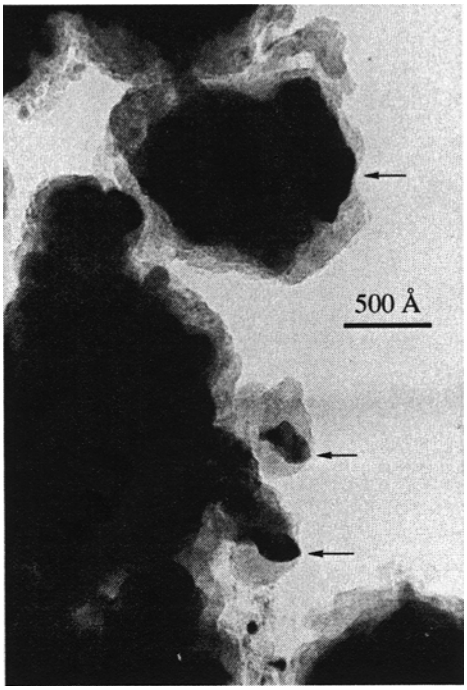

Fig. 2. Carbon at the surface of alloy particles after carbonization of the sample at 350°C. Some regions (marked by arrows) on the surface of alloy particles remain uncovered by carbon.

Carbonization at 450°C. At this temperature, 100% or more carbon was accumulated in the form of carbon fibers that varied in morphology and size. The electron micrographs (Fig. 4) indicate that the morphology of the carbon filaments is closely connected with the particle size of the Ni–Pd alloy. The carbon filaments also differ in the positions of active metal inclusions:

(1) biconical alloy particles are present in the middle of the abundant filaments with a ~1000 Å thickness;

(2) oval alloy particles are present in the middle of the thin (less than 500 Å thick) filaments that are rolled in helical fashion;

(3) in a few filaments with a thickness less than 200 Å, the alloy particles are located at the ends. In each case, the size of metal inclusions nearly coincides with the cross sections of the carbon filaments.

The characteristics of the carbon filaments are determined by the structure of the alloy particles. Let us consider this problem in more detail. The particles of a ~1000 Å size have a biconical symmetrical shape and are elongated in the direction of the growth of the carbon filaments (Figs. 3 and 4). The electron micrographs show that the alloy particles exhibit a block structure as opposed to being single crystals. The presence of satellite reflections and their elongation in the electron microdiffraction pattern are indicative of the occurrence of twins and stacking faults (Fig. 5). The grain boundaries are arranged randomly relative to the symmetry plane of the exterior form of the alloy particle (Figs. 4a and 5). The halves that are symmetrical in morphology are asymmetrical in structure; that is, the right part of a particle is not a structural twin of the left part (in contrast with the results we found for the active particles of the Ni–Cu alloy with a size of 500 Å [15]).

Graphite is formed at conical vertices of the alloy particles, which are turned in different directions. As a result, the two carbon filaments grow in different directions on the alloy particle. The thickness of the carbon layer decreases as the symmetry plane approaches, and

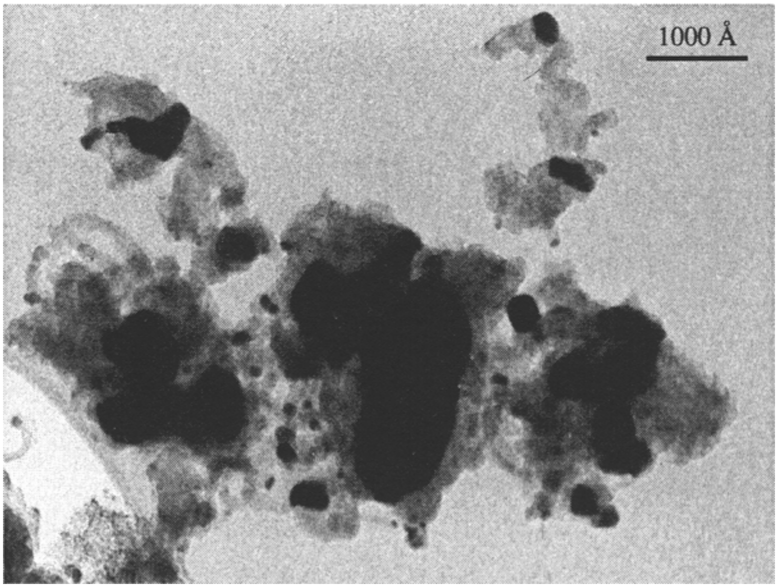

Fig. 3. Carbon formations on the particles of hexagonal nickel in the sample carbonized at 400°C.

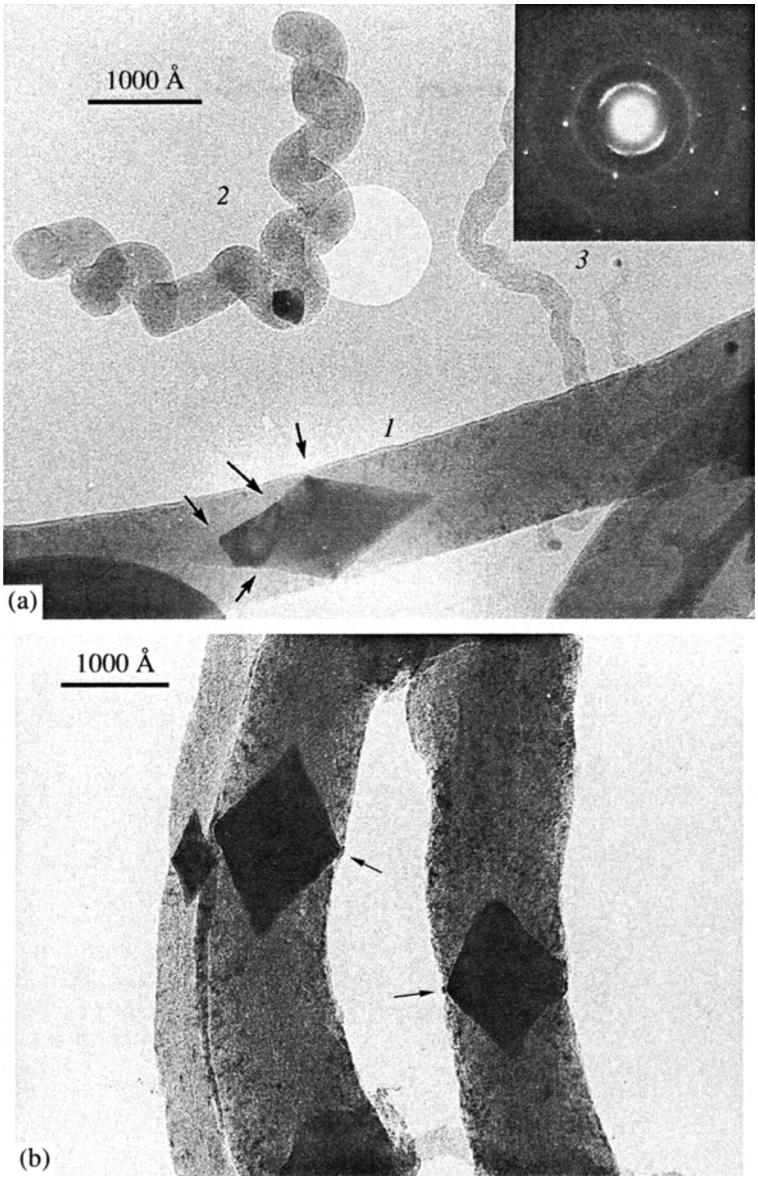

Fig. 4. (a) Electron micrograph of carbon filaments and alloy particles in the sample carbonized at 450 °C: (*1*) a filament with the biconical alloy particle located at the center (the positions of grain boundaries are marked by arrows), (*2*) a symmetrical filament coiled in helical fashion with the oval alloy particle positioned at the center, and (*3*) filaments with alloy particles at the ends. The electron microdiffraction pattern indicating a block structure of the alloy particle and a conical arrangement of carbon layers in the filament is shown in the upper right-hand corner. (b) Electron micrograph of biconical particles of the Ni–Pd alloy in the carbon filaments (marked by arrows).

carbon is completely absent from the region of the surface around the common base of the cones (Figs. 4 and 5). Microphase particles with a characteristic size of about 50 Å were found in this place, which are often in close contact with each other and even form a continuous narrow belt (a width of about 100 Å) around the alloy particle (Figs. 4b, 5, 6). The polycrystalline structure of the belt consisting of microphase particles is clearly seen in the photographs made by high-resolution electron microscopy (HREM), with a direct resolution of the lattice planes (Fig. 6). The interplanar distances of 2.3, 2.2, and 2.0 Å may correspond to the phases of hexagonal nickel or nickel carbide Ni_3C. Nickel carbide is unstable in the temperature range 20–450°C when it is not in contact with the hydrocarbon. Therefore, it is reasonable to expect that the microparticles observed consist of hexagonal nickel formed by decomposing the carbide after cooling the samples. The carbide microphase arises and exists only under the conditions of hydrocarbon decomposition at 450°C and only on a small area of the surface of a Ni–Pd alloy particle due to a strong local supersaturation with carbon.

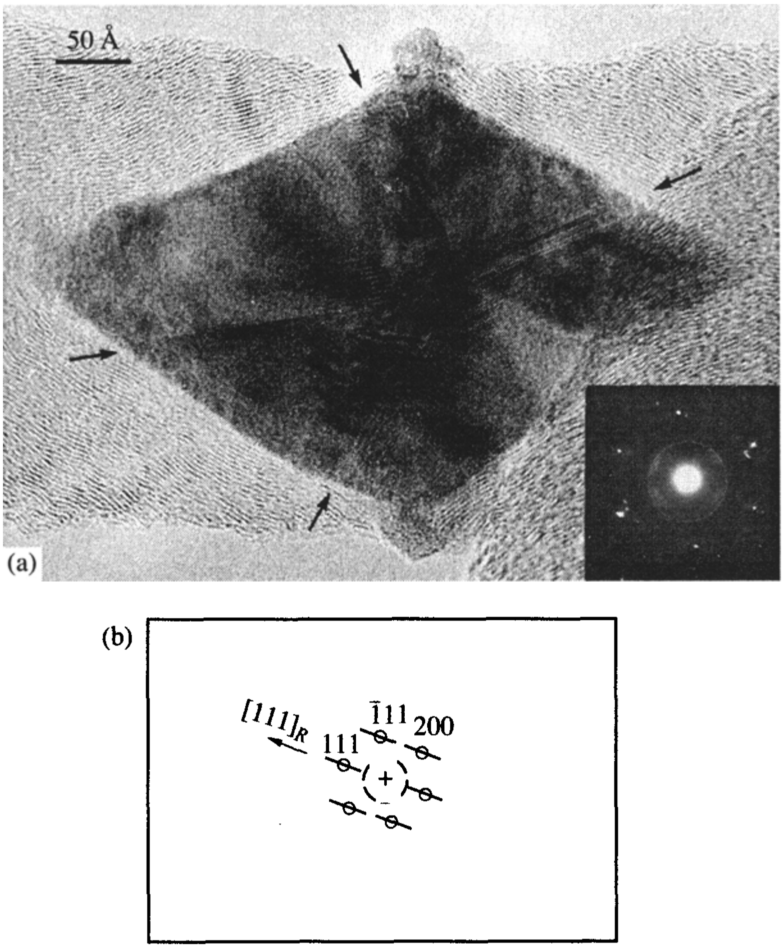

Fig. 5. (a) Nonparallel grain boundaries in the biconical Ni–Pd alloy particle (marked by arrows). The electron microdiffraction pattern of the alloy particle is shown in the bottom right-hand corner. (b) Schematic diagram of the electron microdiffraction pattern presented in Fig. 5a. Satellite reflections are seen along the $[111]_R$ direction, and their extension due to stacking faults in the fcc structure of the Ni–Pd alloy can be observed.

The fast decomposition of the carbide with the formation of carbon atoms, which diffuse through the alloy, inhibits the growth of the bulk carbide. It is obvious that the decomposing nickel carbide that exists only under the reaction conditions is a nonstoichiometric compound and constitutes an intermediate unstable phase whose nature is close to a carbon solution in hexagonal nickel. We will refer to this system as the active phase.

Slightly bent filaments form on the Ni–Pd alloy particles with a size of ~1000 Å, whereas two carbon filaments coiled in helical fashion that diverge symmetrically into opposite directions from the metal particle (Fig. 4a) form on ~500 Å particles. The latter, shaped like an ellipsoid of revolution, flattened toward the direction of carbon filament growth. The structural blocks, twins with randomly oriented grain boundaries, are observed on the HREM patterns of the alloy particles of this size. These particles contain only a single fine particle of the active microphase with a size of 30–50 Å. The microphase particle is located on the side of the alloy particle, and the growing carbon filament begins to bend in the opposite direction immediately upon the "exit" from the metal.

The symmetrical carbon filaments are not formed on small alloy particles (with a size of about 200 Å). The particle of the Ni–Pd alloy arranged at the end of the carbon filament is teardrop-shaped and turned to the growth direction by the cone part.

According to the HREM data, the carbon filaments, regardless of their sizes, are structurally similar and consist of graphene layers, i.e., bent graphite-like networks spaced at a 3.4 Å distance typical of graphite (Figs. 5–7). The mutual arrangement of the layers is determined by the morphology of the alloy particles. A backside of the alloy particle turned to the growing carbon filament has, as a rule, a more or less elongated conical shape. The graphene layers that are distant from the surface of the alloy particle virtually reproduce its conic shape. Because of this, the carbon filament acquires the structure formed by axially symmetrical embedded cones (Fig. 5). Reflection as widened arcs are observed on the electron microdiffraction patterns

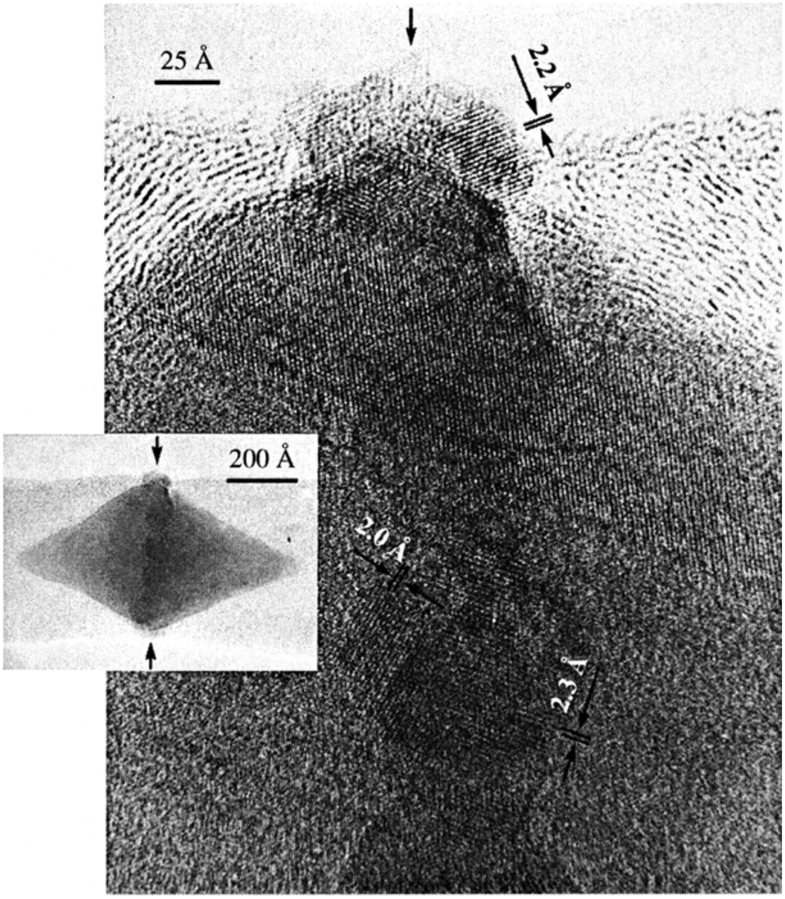

Fig. 6. HREM image of the microphase particles (marked by arrows) surrounding a biconical alloy particle in the middle of a carbon filament.

of these filaments (Fig. 4a), indicating a disordered orientation of the layers on the conic surface to within ±10°.

The above data allow us to draw conclusions on the peculiarities of the carbon filament growth over the Ni–Pd catalyst. We showed earlier [15] that symmetrical twin filaments which emerge from one particle were formed in the course of the carbonization of Ni–Cu alloy particles in 1,3-butadiene at 450°C. On the active microphase of a particle, hydrocarbon decomposes with the formation of a carbide, followed by its decay to the metal and carbon (the carbide cycle mechanism). Under a concentration gradient, the carbon atoms formed rapidly diffuse to the sites of carbon crystallization to a graphite phase. A particle of the nickel carbide microphase acts epitaxially on the bulk of the Ni–Cu alloy and generates a set of mobile twin boundaries that pass through the alloy crystal. During the reaction, the metal changes to a special viscous-flow state. An enhanced ability of crystal lattice atoms to migrate (self-diffusion) arises thanks to a strong supersaturation with carbon and to rapidly passing an intense flow of carbon atoms through the crystal. This leads to strong oscillations of the metal lattice atoms and to the evolution of the heat of carbon condensation from a solution in the metal to the graphite structure of a growing filament. This viscous-flow state is characterized by the high capability of particles to change their shape. The viscous-flow state is similar to a liquid in its properties.

Two types of symmetrical filaments that differ in size and morphology were observed on the Ni–Pd catalysts. The filaments with a thickness of ~ 1000 Å grow from a biconical particle containing the active carbide microphase around the Ni–Pd alloy particle in the base of the cones up to the formation of a narrow polycrystalline belt supersaturated with carbon. The carbon filaments formed on the iron-subgroup metals are generally 500 Å in size. However, thicker filaments (at least 1000 Å) can also form in this case. This is due to the presence of numerous sites of carbon decomposition arranged along the periphery of the bases of adjacent bicones in the particle shortening the diffusion paths of carbon atoms from hydrocarbon decomposition sites to the sites of crystallization to a graphite phase. As in the case of the Ni–Cu catalyst (in which the alloy particle size was 300–500 Å) [15], the particles of the active phase can generate, by the epitaxial action, a hexagonal phase in the alloy that is in the viscous-flow state during

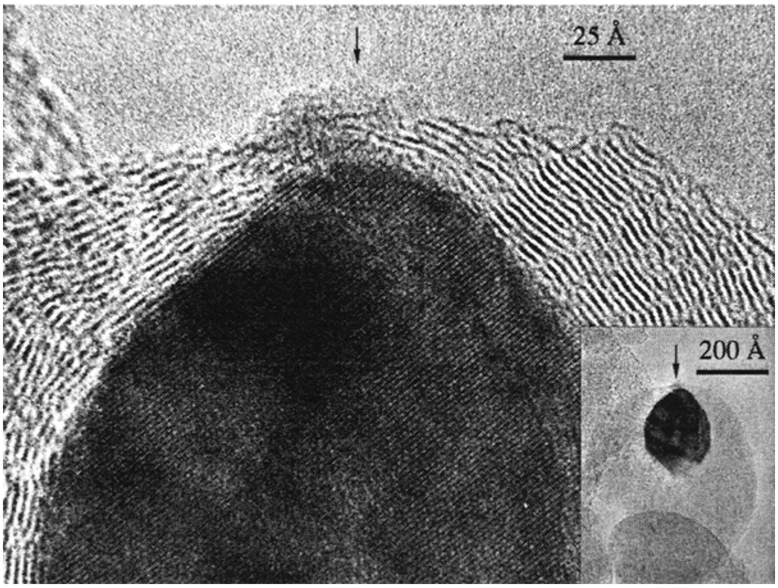

Fig. 7. HREM image of the microphase particle located on the oval alloy particle in the mirror-symmetrical, helically coiled carbon filament.

the reaction. However, unlike Ni–Cu, twin boundaries, which are oriented according to the orientation of each of the numerous microphase particles, are generated on the Ni–Pd alloy particles with a size of ~1000 Å. These grain boundaries can be nonparallel to each other and be oriented randomly in the crystalline alloy.

When the carbon filaments form on smaller particles, carbon atoms produced at the active region have a chance to diffuse to the sites of crystallization to the graphite phase. This condition of a sufficient intensity of the flow of carbon atoms, which originate from one site on the Ni–Pd alloy particle and form the carbon filament, seems to set limits on the filament sizes.

According to the XRD data for the sample carbonized at 400°C, the palladium content of Ni–Pd alloys with both greater and lower Pd contents increases. The alloys are enriched in Pd due to the formation of carbidized nickel containing no palladium in the course of the reaction. In turn, the presence of a noticeable amount of hexagonal Ni is due to the decay of unstable nickel carbide to the metal and carbon upon cooling the sample and its transfer to the XRD camera. At a coking temperature of 450°C, carbide is only present in the form of fine microphase particles on the surface of the Ni–Pd alloy particles and is therefore not observed on X-ray diffraction patterns.

As is known [16], Pd is one of the best hydrogenation catalysts. It is likely that the role of palladium incorporated in the Ni–Pd alloy consists in the acceleration of methanation of both a portion of the atomic carbon formed and of thin layers of graphite in the vicinity of the active phase. As a result of methanation, carbon is removed from the surface of Ni–Pd alloy particles of size 2000 Å, which form a ring around the alloy particle. The surface becomes active in the course of 1,3-butadiene decomposition. It is this surface on which a great number of particles of the metastable active phase form. The methanation of surface carbon also occurs on Ni–Pd alloy particles with sizes of 300–500 Å; however, the reaction only proceeds on a small surface area adjacent to the microphase particle. The appearance of the pure surface of the alloy uncovered by carbon results in the migration of active microphase particles within this free surface. These migrations lead to the generation of twin boundaries from different sites of the surface of the alloy particle by a microphase particle and, thus, to the appearance of nonparallel grain boundaries.

ACKNOWLEDGMENTS

This work was supported by the Russian Foundation for Basic Research (project no. 97-03-32497) and the "Leading Scientific Schools" program (grant no. 96-15-97560).

REFERENCES

1. Buyanov, R.A., Chesnokov, V.V., and Afanas'ev, A.D., *Izv. Sib. Otd. Akad. Nauk SSSR, Ser. Khim. Nauk*, 1981, no. 4, no. 9, p. 28.
2. Buyanov, R.A., *Zakoksovyvanie katalizatorov* (Catalyst Coking), Novosibirsk: Nauka, 1983.
3. Krishnankutty, N., Park, C., Rodriguez, N.M., and Baker, R.T.K., *Catal. Today*, 1997, vol. 37, p. 295.
4. Figueiredo, J.L., Bernado, C.A., Baker, R.T.K., and Huttinger, K.J., *Carbon Fibers, Filaments, and Composites*, Dordrecht: Kluwer, 1990, vol. 177, p. 507.

5. Bernardo, C.A., Alstrup, I., and Rostrup-Nielsen, J.R., *J. Catal.*, 1985, vol. 96, p. 517.
6. Van Stiphout, P.C.M., Stoble, D.E., Scheur, F.Th.V.D., and Geus, J.W., *Appl. Catal.,* 1988, vol. 40, p. 219.
7. Alstrup, I., *J. Catal.*, 1988, vol. 109, p. 241.
8. Chesnokov, V.V., Zaikovskii, V.I., Buyanov, R.A., *et al.*, *Kinet. Katal.*, 1994, vol. 35, no. 1, p. 146.
9. Buyanov, R.A. and Chesnokov, V.V., *Zh. Prikl. Khim.*, 1997, vol. 70, no. 6, p. 978.
10. Lipson, H. and Steeple, H., *Interpretation of X-ray Powder Diffraction Patterns,* London: Macmillan, 1970.
11. Guinier, A., Theorie et technique de la radiocristallographie, Paris, 1956.
12. Mintsa-Eya, V., Hilaire, L., Touroude, R., *et al.*, *J. Catal.*, 1983, vol. 76, p. 169.
13. Chesnokov, V.V., Buyanov, R.A., and Afanas'ev, A.D., *Izv. Sib. Otd. Akad Nauk SSSR, Ser. Khim. Nauk*, 1982, no. 2, no. 4, p. 60.
14. Nagakura, S., *J. Phys. Soc.*, 1957, vol. 12, no. 5, p. 482.
15. Zaikovskii, V.I., Chesnokov, V.V., and Buyanov, R.A., *Kinet. Katal.,* 1999, vol. 40, no. 4, p. 612.
16. Zanozina, P.P., Sokol'skii, D.V., and Zhanabaev, B.Zh., *Adsorbtsiya i gidrogenizatsiya arenov na metallakh VIII gruppy* (Adsorption and Hydrogenation of Arenes over Group VIII Metals), Alma-Ata: Nauka, 1985.